Estimating the optimal sampling rate using wavelet transform: an application to optical turbulence

Gustavo Funes,[1,*] **Ángel Fernández,**[2,3] **Darío G. Pérez,**[2] **Luciano Zunino,**[1,4] **and Eduardo Serrano**[5]

[1]*Centro de Investigaciones Ópticas (CONICET La Plata - CIC), C.C. 3, 1897 Gonnet, Argentina*

[2]*Instituto de Física, Pontificia Universidad Católica de Valparaíso (PUCV), 23-40025 Valparaíso, Chile*

[3]*Departamento de Física, Universidad Técnica Federico Santa María (UTFSM), 23-90123 Valparaíso, Chile*

[4]*Departamento de Ciencias Básicas, Facultad de Ingeniería, Universidad Nacional de La Plata (UNLP), 1900 La Plata, Argentina*

[5]*Centro de Matemática Aplicada, Universidad Nacional de San Martín, 1650 San Martín, Argentina*

[*] *gfunes@ciop.unlp.edu.ar*

Abstract: Sampling rate and frequency content determination for optical quantities related to light propagation through turbulence are paramount experimental topics. Some papers about estimating properties of the optical turbulence seem to use *ad hoc* assumptions to set the sampling frequency used; this chosen sampling rate is assumed good enough to perform a proper measurement. On the other hand, other authors estimate the optimal sampling rate via fast Fourier transform of data series associated to the experiment. When possible, with the help of analytical models, cut-off frequencies, or frequency content, can be determined; yet, these approaches require prior knowledge of the optical turbulence. The aim of this paper is to propose an alternative, practical, experimental method to estimate a proper sampling rate. By means of the discrete wavelet transform, this approach can prevent any loss of information and, at the same time, avoid oversampling. Moreover, it is independent of the statistical model imposed on the turbulence.

References and links

1. V. I. Tatarskĭ, *Wave Propagation in a Turbulent Atmosphere* (Nauka Press, Moscow, 1967).
2. H. T. Yura, "Physical model for strong optical-amplitude fluctuations in a turbulent medium," J. Opt. Soc. Am. **64**, 59–67 (1974).
3. A. Ishimaru, *Wave Propagation and Scattering in Random Media* (IEEE Press & Oxford University Press, 1997).
4. L. C. Andrews and R. L. Phillips, *Laser Beam Propagation through Random Media* (SPIE, 1998).
5. R. L. Fante, "Mutual coherence function and frequency spectrum of a laser beam propagating through atmospheric turbulence," J. Opt. Soc. Am. **64**, 592–598 (1974).
6. S. F. Clifford, "Temporal-frequency spectra for a spherical wave propagating through atmospheric turbulence," J. Opt. Soc. Am. **61**, 1285–1292 (1971).

7. D. P. Greenwood, "Bandwidth specification for adaptive optics systems," J. Opt. Soc. Am. **67**, 390–393 (1977).

8. G. A. Tyler, "Bandwidth considerations for tracking through turbulence," J. Opt. Soc. Am. A **11**, 358–367 (1994).

9. L. R. Bissonnette, "Atmospheric scintillation of optical and infrared waves: a laboratory simulation," Appl. Opt. **16**, 2242–2251 (1977).

10. A. Consortini, C. Innocenti, and G. Paoli, "Estimate method for outer scale of atmospheric turbulence," Opt. Commun. **214**, 9–14 (2002).

11. V. P. Lukin and V. V. Pokasov, "Optical wave phase fluctuations," Appl. Opt. **20**, 121–135 (1981).

12. N. Ben-Yosef and E. Goldner, "Sample size influence on optical scintillation analysis. Analytical treatment of the higher-order irradiance moments," Appl. Opt. **27**, 2167–2171 (1988).

13. F. Martin, A. Tokovinin, A. Agabi J. Borgnino, and A. Ziad, "G.S.M.: a Grating Scale Monitor for atmospheric turbulence measurements. I. The instrument and first results of angle of arrival measurements," Astron. Astrophys. Sup. **108**, 173–180 (1994).

14. F. S. Vetelino, B. Clare, K. Corbett, C. Young, K. Grant, and L. Andrews, "Characterizing the propagation path in moderate to strong optical turbulence," Appl. Opt. **45**, 3534–3543 (2006).

15. H. T. Yura and D. A. Kozlowski, "Low Earth orbit satellite-to-ground optical scintillation: comparison of experimental observations and theoretical predictions," Opt. Lett. **36**, 2507–2509 (2011).

16. J. A. Anguita and J. E. Cisternas, "Influence of turbulence strength on temporal correlation of scintillation," Opt. Lett. **36**, 1725–1727 (2011).

17. L. Kral, I. Prochazka, and K. Hamal, "Optical signal path delay fluctuations caused by atmospheric turbulence," Opt. Lett. **30**, 1767–1769 (2005).

18. L. P. Poggio, M. Furger, A. H. Prévôt, W. K. Graber, and E. L. Andreas, "Scintillometer Wind Measurements over Complex Terrain," J. Atmos. Oceanic Technol. **17**, 17–26 (2000).

19. G. Potvin, D. Dion, and J. L. Forand, "Wind effects on scintillation decorrelation times," Opt. Eng. **44**, 016001 (2005).

20. S. Mallat, *A Wavelet Tour of Signal Processing* (Academic Press, Elsevier, 2009).

21. D. Percival and A. Walden, *Wavelet Methods for Time Series Analysis*, Cambridge Series In Statistical And Probabilistic Mathematics (Cambridge University Press, 2006).

22. C. K. Chui, *An Introduction to Wavelets* (Academic Press, 1992).

23. M. Farge, "Wavelet transforms and their applications to turbulence," Annu. Rev. Fluid Mech. **24**, 395–457 (1992).

24. L. Hudgins, C. A. Friehe, and M. E. Mayer, "Wavelet transform and atmospheric turbulence," Phys. Rev. Lett. **71**, 3279–3282 (1993).

25. D. G. Pérez, A. Fernandez, G. Funes, D. Gulich, and L. Zunino, "Retrieving atmospheric turbulence features from differential laser tracking motion data," SPIE Proc. **8535** (2012).

26. O. Keskin, L. Jolissaint, and C. Bradley, "Hot-air optical turbulence generator for the testing of adaptive optics systems: principles and characterization", Appl. Opt. **45**, 4888–4897 (2006).

27. S. Blanco, A. Figliola, R. Quian Quiroga, O. A. Rosso, and E. Serrano, "Time-frequency analysis of electroencephalogram series. III. Wavelet packets and information cost function," Phys. Rev. E **57**, 932–940 (1998).

1. Introduction

Frequency content of fluctuations of lightwave parameters in turbulent media was first determined by Tatarskĭ [1]. By using the *frozen turbulence hypothesis* and the Obukhov-Kolmogorov (OK) model, he showed that the phase and amplitude frequency spectra of a wave propagating through turbulent media span up to a frequency that linearly depends on the mean transverse flow velocity. Further extensions were obtained [2–5], considering more elaborated models, but valid within the weak turbulence regime, i.e., when the Rytov variance is much less than one, $\sigma_R^2 \ll 1$. The strong regime has received far less attention, only the log-amplitude covariance [2, 4] has been studied for plane waves, and the effects of finite inner- and outer-scales have been ignored.

As the Nyquist-Shannon sampling theorem asserts, sampling rate is directly related to the frequency content; therefore, any experiment should warrant that all the relevant frequencies of the observed quantities are included for the chosen sampling rate. In the last decades several authors have performed experiments to measure fluctuations in lightwave parameters, but the choice of a sampling rate is sometimes unclear.

The pioneering works of Yura [2] and Clifford *et al.* [6] were some of the first to establish frequency bandwidths for the scintillation and phase, respectively. Later works [7–16] have obtained, for these and other optical quantities, different cut-off frequencies; thus, specify-

ing an optimal sampling rate, f_s, for each particular situation. Experimentally, sometimes its choice is unjustified, or there are technical limitations precluding its selection (sampling frequency limits on the measurement device or detector, lack of computing power, etc.). Whereas in theoretical works, the obtained frequency strongly depends on the measurements of turbulence characteristics (inner and outer scales, structure constant, mean wind profiles, etc.). Ultimately, the frequency content due to the optical turbulence depends on the experimental arrangement, and the turbulence characteristics mentioned before. Some authors have estimated, through the fast Fourier transform (FFT), that the spectral range of turbulence extends from 20 to 200Hz [12, 17]; but these values are directly related to their experiments.

Another consideration of interest when searching for frequency content, or other relevant quantities, is that theoretical models are not always capable of reproducing temporal series of optical quantities. For instance, scintillation measurements in astronomic sites have revealed systematic fails in the estimation of cross winds during calm nights [18]; surface-layer measurements also show scintillation discrepancies even after including longitudinal winds contributions [19]. That is how, sometimes, scintillation theory is unable to offer a clean model for the temporal spectra. Therefore, simpler exponential models (that differ from any known theory) [16] have been employed.

2. Wavelet method

Wavelet analysis was first introduced in seismology to provide a temporal scale to seismic data, since Fourier analysis was unable to cope with transient events [20]. Wavelets were used ever since in various fields with very good performance for non-stationary signal analysis and processing. The idea of using the wavelet transform to study fluid turbulence was originally introduced by Farge [23]. Fourier transform decomposes signals through plane waves, thus it is specially suited for periodic or non-localized stationary data. As turbulent data seem to be composed of coherent structures with a well-defined scale hierarchy, wavelets naturally become more appropriate to study it. The wavelet transform allows the analysis of intermittent behaviour commonly present in turbulent signals. This is possible since it yields scale-time information, while the Fourier transform is only able to show the frequency content of the signal. Hudgins *et al.* [24] developed a Fourier equivalent Wavelet Cross Spectrum. By applying this approach to turbulent experimental data, they proved that the scale-time properties of the wavelets go beyond the FFT capabilities.

The *discrete wavelet transform* (DWT, or Mallat Algorithm) decomposes a signal into low- and high-frequency components by convolution with low- and high-pass filters, respectively. These filters are generated from a special function of compact support, called *the mother wavelet*—see [20] for definitions. This procedure divides the signal in two parts: the global features are kept by low-frequency components, *approximation coefficients*, whereas the local features are retained by the high-frequency ones, *detail coefficients*. The second decomposition level takes the *approximation coefficients* and starts the convolution again. This tree conforms the multiresolution analysis [22]. The decomposition can be done N times being 2^N the length of the signal. The DWT can be defined as a matrix product

$$W = \widetilde{W} \otimes S, \tag{1}$$

where S represents the signal as a column vector, $\widetilde{W}$ is a matrix containing all dilations and translations of the mother wavelet, and W is the wavelet transform. The last one is a column matrix composed of all wavelet coefficient $C_J(k)$ from all level decompositions (J) and all times (k). Since the DWT is an ortonormal transform, it permits to establish an energy preserving condition [21]

$$\|S\|^2 = \|W\|^2 = \sum_{J,k} C_J(k)^2. \tag{2}$$

This condition makes the DWT particularly useful in estimating the normalized energy content per frequency bands: the *wavelet energy spectrum* (WES). This provides a fast and practical visualization of the frequency content; that is, an estimation of the optimal sampling rate. The scale band frequency employed in the wavelet decomposition for the WES is defined by a dyadic scaling of the sampling rate

$$f_J = 2^J f_s, \tag{3}$$

where J goes from $J_{\min}$ to -1, with $J_{\min}$ determined by the length of the signal to be analysed ($J_{\min} = -N$). In general, each band is composed of frequencies from $2^{(J-1)} f_s$ to $2^J f_s$—for example, the $J = -1$ band contains frequencies from $2^{-2} f_s$ to $2^{-1} f_s$. The WES is obtained by evaluating the following equation:

$$E_J = \frac{\sum_k C_J(k)^2}{\sum_{J,k} C_J(k)^2}, \tag{4}$$

where k is the sampling time index. In general the DWT is a versatile tool for extracting features and information from any given signal. For instance, the detail coefficients can be examined by bands to detect transient events, or specific denoising algorithms can be applied to eliminate spurious noise. Also, the approximation coefficients can be used to find trends—see Sec. 3.

The *power spectral density* (PSD) is the Fourier analogue to the WES. Usually, the determination of the sampling rate through the PSD is bound to an arbitrary criterion, e.g.: locating the frequency at which 90% of the power is contained, and then estimating the sampling rate as twice this frequency (Nyquist). Alternatively, the inverse of the cross-temporal correlation's half-life time can provide another estimate. Although arbitrary, these criteria are still very powerful tools. And the Fourier transform also provides a strong analytical framework. Unfortunately, The results derived by using it are only valid for stationary series. The optical turbulence (like many natural phenomena) is prominently non-stationary; therefore, a criterion based on the wavelet energy spectrum should be more robust. Naturally, it presents a significant fraction of energy located in those bands where the turbulent phenomenon is more active. We particularly argue that if the highest band ($J = -1$) is quite different from zero, some activity may be missing—the spectrum may appear slashed. That is, there are unaccounted for features at higher frequencies disregarded by the actual sampling rate: the recorded data is undersampled.

3. Experiment & discussion

To demonstrate this procedure we have performed a conceptually simple experiment of laser propagation through turbulent media at different sampling rates (0.8, 2, 6, and 12 kHz). Basi-
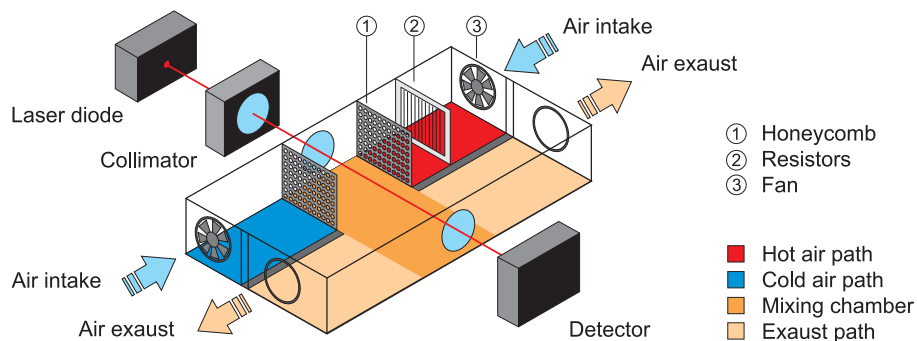

Fig. 1. Experimental setup.

cally, it consists in the propagation of a collimated Gaussian thin beam ($1/e^2$ diameter of 3mm) through artificial turbulence (Fig. 1). For the purpose of having isotropic turbulence at stable conditions we employ a device similar to the one described in [26], the *turbulator*: two air fluxes at different temperatures collide in a chamber producing an isotropic mix between hot and cold sources. The beam propagates along forty centimeters of turbulence, with an estimated inner-scale of 6mm [25], before exiting. Then, it impinges on the surface of a position sensor detector, where its horizontal and vertical displacements are recorded. The experience is dynamic, but the first 20 seconds consist of keeping the hot air flow at room temperature. Afterwards, the temperature difference between the two fluxes is increased. When reached the highest temperature possible, the cooling process is achieved by lowering the temperature at the hot flow. A continuous measurement of seven and a half minutes is obtained. Although, temperature differences up to 150°C are achieved, the turbulence is weak, with $\sigma_R^2 = 0.02$ and structure constant $C_n^2 = 6 \times 10^{-10}$ m$^{-2/3}$ at its highest point ($\sigma_R^2 = 0.003$ and $C_n^2 = 9 \times 10^{-11}$ m$^{-2/3}$ at the end of the experiment). The Rytov index was obtained from the long-term beam spot size observed from the wandering data, according to [4, Eq. (46), p. 189]. Air flow velocity is fixed so the turbulence characteristics are only due to the temperature difference.

In order to analyse the recorded data we use the DWT algorithm with a Haar basis, this is the simplest mother wavelet. It is very well localized in time, but poorly in frequency, thus making it well suited to detect sudden changes. Computationally, it has been proven to be fast when examining large amount of data. Because of the disadvantage of the Haar basis, we have also estimated the WES with other wavelet basis for some reference data series and found no major discrepancies; therefore, the use of more complex mother wavelets is unjustified for our purposes. The wavelet spectrum for different sampling rates for horizontal displacements can be observed in Fig. 2—the vertical displacements behave alike and would not be shown here. At the beginning of the experiment the WES shows a maximum of energy around the highest frequency bands; this is related to spurious noise caused by the detector. As the experiment
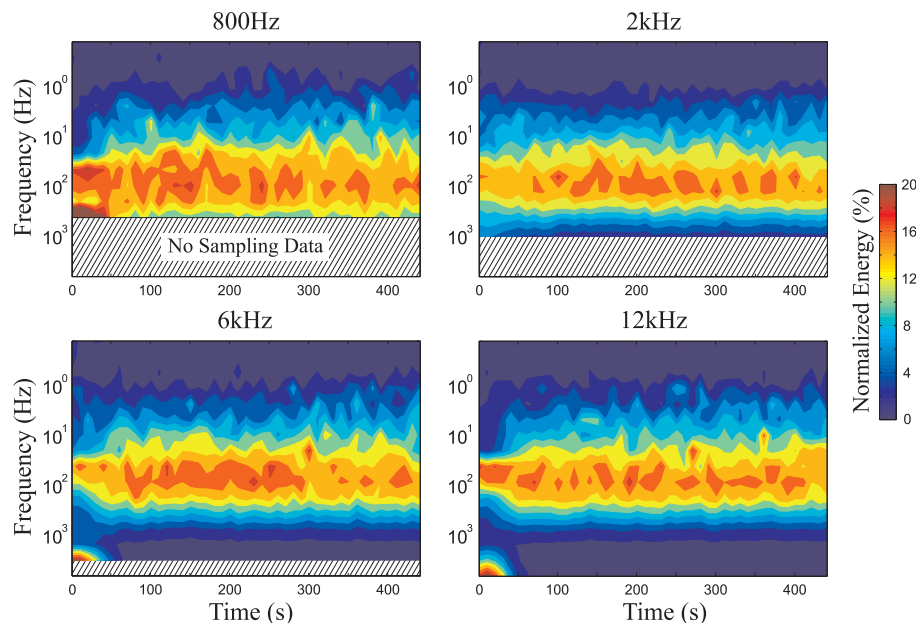

Fig. 2. Density plots of the WES for the horizontal displacements for different sampling rates showing the temporal evolution.

progresses the frequency content related to the turbulence becomes predominant; signal to noise ratio increases, and this peak vanishes.

The energy distribution per frequency remains constant: the bell-shaped WES is centered around the same frequency bands. This is in good agreement with theoretical results since the flow velocity is fixed [1, 4]. Figure 3 shows the comparison between the estimated WES and PSD for the same data series at a given sampling rate, again for horizontal displacements, at time index around 80s. The very first two wavelet spectra obtained (at 0.8 and 2kHz) present considerable contribution to the energy at the highest frequency bands: there is missing information from the turbulence under study. Although for the second in a lesser extent, both sampling rates can be considered as improper since the original signal is undersampled, and our aim is to have a complete view of the frequency spectrum. On the other hand, the measure-
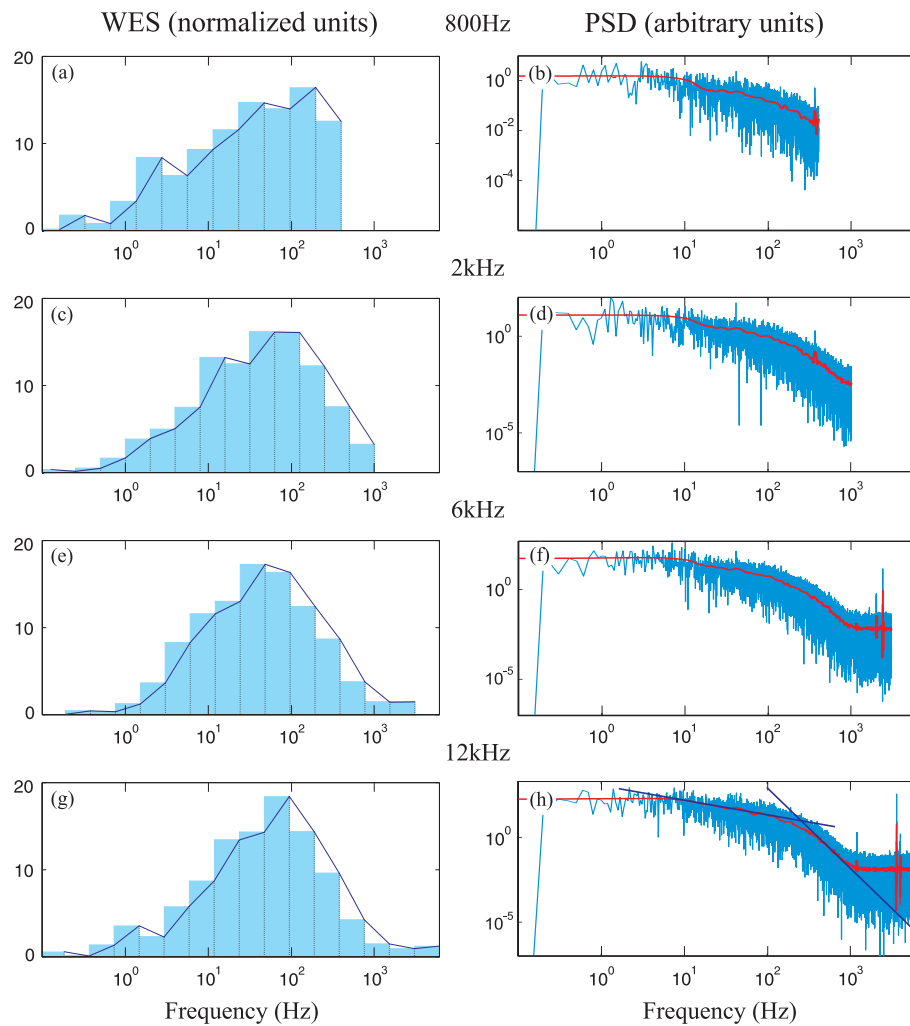

Fig. 3. a) WES and b) PSD at a sampling rate of 800Hz, c) and d) idem for 2kHz, e) and f) idem for 6kHz, g) and h) idem for 12kHz. For the wavelet spectra the frequency bands were marked. The red curve is the thrend of the PSD obtained via wavelets. Also, the theoretical Kolmogorov slopes $-2/3$ and $-11/3$ are shown in h).

ments performed at 6 and 12kHz clearly provide full information of the horizontal wandering. Therefore, a lower bound for the sampling frequency should be around 3kHz. A higher sampling frequency is unnecessary since it would carry no new information about the turbulence, thus we are avoiding oversampling. Finally, as the sampling rate increases, the PSD (Fig. 3, left column) reveals the occurrence of a knee around 1kHz. It is unclear if the turbulence ceased to be active or the signal-to-noise ratio is too low at high frequencies. Either way, what naturally appears in the WES would require a deeper inspection of the PSD—if a theoretical model is unavailable, a proper determination of the bandwidth maybe a hard task.

4. Conclusions

Since the outlined wavelet approach is independent of any theoretical model, it can be extended rather easily to any other experimental settings. For example, in the case of adaptive optics, it could allow the determination of frequency content without any prior knowledge of the structure constant nor wind velocity profiles. Generally, data obtained from turbulence in any dynamic state (inertial, anisotropic, convective, etc.), whether it is strong or weak, can be studied as well. Specifically, those instances where theoretical models are unavailable or primary hypotheses, like stationarity or frozen-in turbulence, fail.

Two main considerations should be used to determine an optimal sampling rate from the WES: the bell-shaped energy distribution corresponding to the optical turbulence must be completely visible for a given f_s; and the lowest and highest bands, associated to mechanical and electronic noise, should have a negligible signature in the spectrum—compare the temporal evolution of the WES in Fig. 2 for 6 and 12kHz. Under these conditions we can obtain a practical estimation of the optimal sampling rate without losing any information regarding the original dynamics. The advantage of this method is twofold; it permits to isolate noise from signal and be applied indistinctly to both stationary and non-stationary series. Furthermore, this procedure is independent from any theoretical model or ad hoc hypotheses regarding the optical turbulence. Finally, even though this approach is highly qualitative, it has proven to be fast and effective; therefore, our future objective is to improve it by using more complex wavelet transforms such as the wavelet packets [27]. This will allow us to identify the dominant frequencies in a more accurate way, and reduce any possible subjectivity in the optimal sample rate estimation.